A Novel Position Control of PMSM Based on Active Disturbance Rejection

XING-HUA YANG, XI-JUN YANG, JIAN-GUO JIANG
Dept. of Electrical Engineering, Shanghai Jiao Tong University,
200240, Shanghai, CHINA
yangxinghua2004@126.com

Abstract: - Considering the unavoidable and unmeasured disturbances, parameter variations and position measure error of real motion control applications, a novel controller is developed for the motion control of permanent-magnet synchronous motors (PMSM). First, an active disturbance rejection controller (ADRC) based on extended state observer (ESO) is employed to ensure the high performance of the entire control system. The ESO estimate both the states and the disturbances so that the ADRC has a corresponding part to compensate for the disturbances. And then, the inertia of system is identified online to improve the performance. At last, considering the case of position measure error, which is commonly in the applications that an encoder is used for position detection, an asynchronous sampling method (ASM) is used. The ASM detects the position at the moment of actual encoder pulse input, thus eliminating encoder positioning error. Simulation and Experimental results are shown to verify the method.

Key-Words: - Permanent-magnet synchronous motors, Active disturbance rejection controller, Extended state observer, Asynchronous sampling method, Inertia identification.

1 Introduction

Motion control applications can be found in almost every sector of industry, from factory automation and robotics to high-tech computer hard-disk drives. Permanent magnet synchronous motors (PMSM), which possess the characteristics of high power density, torque/inertia, efficiency, and inherent maintenance-free capability, have been recognized as one of the key components in motion control applications.

Conventionally, PID control is already widely applied in the PMSM system due to its relative simple implementation. Over the years, many researchers have developed various tuning methods for the ease of application[1-5]. However, the PMSM system is a nonlinear system with unavoidable and unmeasured disturbances, as well as parameter variations. This makes it very difficult for PID control algorithm to obtain a sufficiently high performance for this kind of nonlinear systems in the entire operating range.

Recently, with the rapid progress in micro-processors and modern control theories, many researchers have contributed their efforts toward nonlinear control algorithms, and various algorithms have been proposed, e.g., adaptive control[6, 7], robust control[8-10], sliding mode control[11, 12], input-output linearization control[13], back-stepping control[14, 15], and intelligent control[16, 17]. These algorithms have improved the control performance of PMSM from different aspects.

However, in real industrial applications, PMSM systems are always confronted with different disturbances, e.g., friction force, unmodeled dynamics and load disturbances. Conventional feedback-based control methods usually cannot react directly and fast to reject these disturbances, although these control methods can finally suppress them through feedback regulation in a relatively slow way.

Since it is usually impossible to measure the disturbances directly, one efficient way of improving system performance in such cases is to develop an observer to estimate the disturbances. The disturbances observers offer several attractive features. In the absence of large model errors, they allow independent tuning of disturbances rejection characteristics and command-following characteristics[18-21]. Further, compared to integral action, disturbances observers allow more flexibility via the selection of the order, relative degree, and bandwidth of low-pass filtering.

Another kind of disturbance rejection techniques is active disturbance rejection control (ADRC), which is proposed by Jinqing Han[22]. The ADRC is designed without an explicit mathematical model of the plant. Hence the controller is inherently robust against plant variations. Generally the ADRC

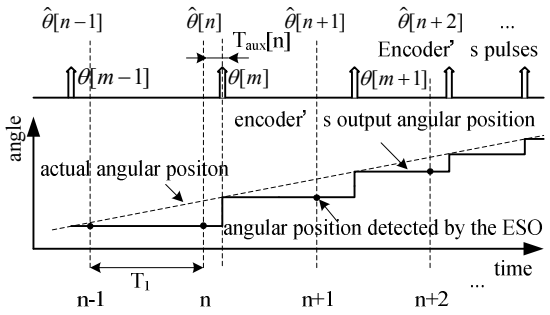

Fig.1 Timing diagram of angular position measurement

consists of three parts: Tracking Differential (TD), Extended State Observer (ESO) and Nonlinear State Error Feedback control law (NLSEF). The ESO regards the total disturbances of the system, which consists of internal dynamics and external disturbances, as a new state of the system. This observer is one order more than the usual state observer. It can estimate both the states and the total disturbances. Based on the ESO, a feed forward compensation for the disturbances can be employed in the control design. Then ADRC compensates the system parameter disturbance of the model, suppresses the disturbance outside the system at the same time.

However, accuracy measurement of angular position is vital for the implementation of ESO. In the real motion control applications, incremental encoders are popular for detecting angular position. Since the angular position is only available at the moment of encoder pulse input, there are positioning error and detection delay between the actual angular position and that detected by the ESO (as shown in Fig.1). When the system operates in the low speed range, the positioning error and detection delay will deteriorate the performance of the ESO as well as the entire control system.

In order to suppress the effect of disturbances, parameter variations and measurement error of angular position on motion control system, a novel controller is developed in this paper. First, a linear ADRC based on ESO is employed to ensure the high performance of the entire control system. Then, for the purpose of obtaining angular position precisely in the situation of low speed, an asynchronous sampling method (ASM) is employed. Mathematical model of PMSM system is given in Section2. The principle of ESO-based linear ADRC is described in Section 3. The detail implementation of ESO with asynchronous angular position sampling is discussed in Section 4.

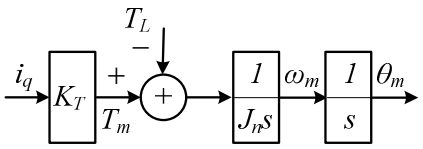

Fig.2 Block diagram mechanical model of PMSM motion control system

2 Model of PMSM System

The block diagram mechanical model of PMSM motion control system is shown in Fig.2. The motion equation in the motor side can be written as below,

$$\frac{d\theta_m}{dt} = \omega_m \tag{1}$$

$$J_n \frac{d\omega_m}{dt} = T_m - T_L \tag{2}$$

$$T_L = f(\omega_m, J_L) \tag{3}$$

where

θ_m -the mechanical angular position

ω_m - the mechanical angular velocity

J_n -the total inertial moment of system, including the moment of PMSM J_m and that of load J_L

T_M -the developed torque

T_L -the disturbance torque

Normally, the disturbance torque T_L varies with the change of load and working conditions. It is unavoidable and immeasurable.

PMSM is a complex nonlinear system with multivariables and strong coupling. In order to reduce the analysis, the saturation and damping effects are neglected. A schematic of the PMSM motion control system based on vector control is shown in Fig.3. As shown in Fig.3, two PI algorithms are used in the two current loops, respectively. Under the field-oriented vector control scheme, the torque- and flux-producing components of the stator current are decoupled so that the independent torque and flux controls are possible as in dc motors. Usually, the d-axis current reference i_d^* is set to be $i_d^*=0$ in order to approximately eliminate the couplings between angular velocity and currents. Assuming that the current controllers are properly designed and the controller for d-axis current loop works well, the output i_d satisfies $i_d=i_d^*=0$. Then the d-axis flux linkage is fixed and the developed torque T_m is then proportional to q-axis current i_q, which is determined by closed-loop control.

$$T_m = K_T i_q \tag{4}$$

where K_T is the torque coefficient.

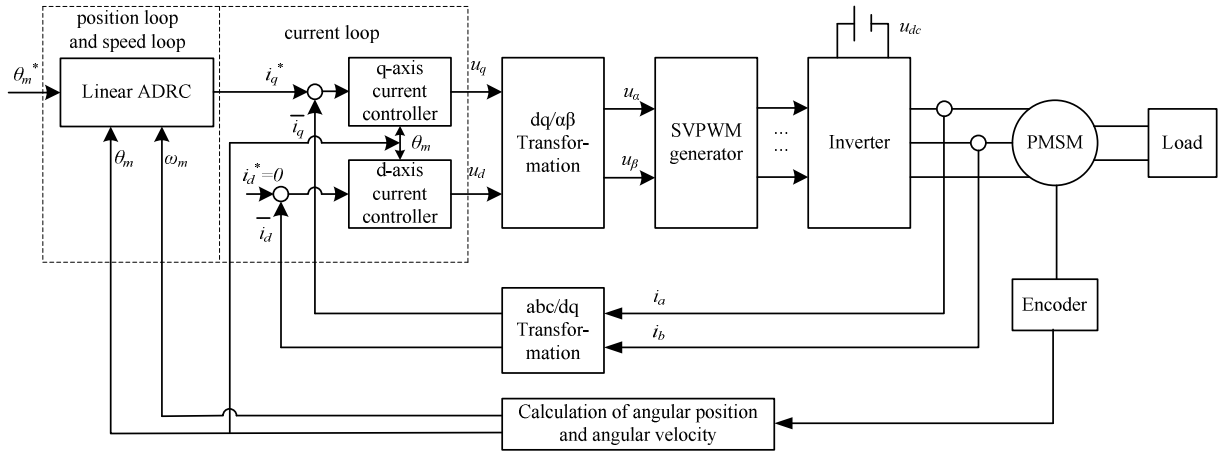

Fig.3 Schematic diagram of the PMSM motion control system

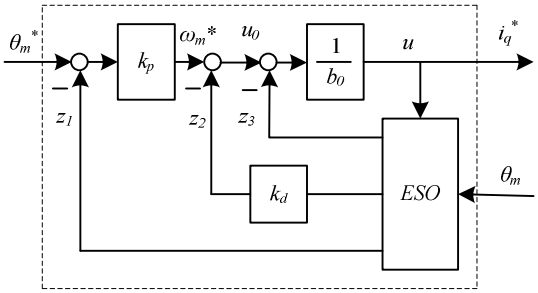

Fig.4 Block diagram of the linear ADRC based on ESO

3 ADRC for PMSM System

A linear active disturbance rejection controller (ADRC) is introduced to achieve high dynamic performance in the overall operating range. It is composed of two parts (shown in Fig. 4): 1) extended state observer (ESO), and 2) linear state error feedback control law. The essential part of ADRC is the extended state observer.

3.1 Extended State Observer

The ESO is a configuration for observing the states and disturbances of the system under control without the knowledge of the exact system parameters. Unlike the full order (*N* th order) state observer, ESO utilizes *N+1*th order (full order plus 1) state observation to achieve state and disturbance estimation. The total disturbances in PMSM system include external disturbances such as load variation and internal uncertainties such as the modelling errors.

For the PMSM motion control system, considering parameter variations as well as unavoidable and unmeasured disturbance torque T_L, (2) can be rewritten as

$$\frac{d\omega_m}{dt} = a(t) + b_0 i_q^* \tag{5}$$

where

$$a(t) = -\frac{T_L}{J_n} + \frac{K_T}{J_n}\left(i_q - i_q^*\right) + \left(\frac{K_T}{J_n} - b_0\right) i_q^*$$

represents external disturbance torque, the tracking error of the current loop of i_q, and the modeling error. Note that b_0 is an estimate of K_t/J_n. The disturbance $a(t)$ is unmeasurable and time-variant.

Regard disturbance $a(t)$ as an extended state and let $da(t)/dt=h$, with h unknown. Define $x_1 = \theta_m$, $x_2 = \omega_m$, $x_3 = a(t)$, $y = \theta_m$, $u = i_q^*$, then the state equations of PMSM system are given by

$$\begin{cases} \dot{\mathbf{x}} = \mathbf{A}\mathbf{x} + \mathbf{B}u + \mathbf{E}h \\ y = \mathbf{C}\mathbf{x} \end{cases} \tag{6}$$

where

$$\mathbf{A} = \begin{bmatrix} 0 & 1 & 0 \\ 0 & 0 & 1 \\ 0 & 0 & 0 \end{bmatrix}, \quad \mathbf{B} = \begin{bmatrix} 0 \\ b_0 \\ 0 \end{bmatrix}, \quad \mathbf{C} = \begin{bmatrix} 1 & 0 & 0 \end{bmatrix}, \quad \mathbf{E} = \begin{bmatrix} 0 \\ 0 \\ 1 \end{bmatrix}$$

In the PMSM motion control system, angular position can be detected by encoder. Based on the plant model (6) and real output angular position from the plant, the linear ESO of PMSM is constructed as[23]

$$\begin{cases} \dot{\mathbf{z}} = \mathbf{A}\mathbf{z} + \mathbf{B}u + \mathbf{L}\left(y - \hat{y}\right) \\ \hat{y} = \mathbf{C}\mathbf{z} \end{cases} \tag{7}$$

where $\mathbf{z}$ is an estimate of state $\mathbf{x}$, $\mathbf{L}$ is the observer gain vector,

$$\mathbf{L} = \begin{bmatrix} l_1 & l_2 & l_3 \end{bmatrix}^T \tag{8}$$

Assume the poles of the ESO (7) are p_1, p_2 and p_3 (p_1, p_2, p_3<0). So the obserer gains can be calculated by

$$l_1 = p_1 + p_2 + p_3 \tag{9}$$

$$l_2 = p_1 p_2 + p_2 p_3 + p_1 p_3 \tag{10}$$

$$l_3 = p_1 p_2 p_3 \tag{11}$$

Define the estimation error $e_i = x_i - z_i$, $i=1, 2, 3$, and the error equation can be written as

$$\dot{\mathbf{e}} = \mathbf{A}_e \mathbf{e} + \mathbf{E}h \tag{12}$$

where

$$\mathbf{A}_e = \mathbf{A} - \mathbf{L}\mathbf{C} = \begin{bmatrix} -l_1 & 1 & 0 \\ -l_2 & 0 & 1 \\ -l_3 & 0 & 0 \end{bmatrix}$$

If the roots of the characteristic polynomial of $\mathbf{A}_e$ are all in the left half plane and h is bounded, the ESO (7) is bounded-input bounded-output stable [23]. In the PMSM motion control system, although the disturbance, $a(t)$, is not measurable, it varies continuously. So the derivation of the disturbance, h, is always bounded.

The remaining issue is to properly design the observer gain vector, L, to satisfy the performance of ESO. There are many methods used to obtain L, such as the pole placement technique. It is important to note that a proper selection of the gains in (7) is critical to the success of the observer. The ESO must be stable firstly, or it would cause the whole system to be unstable. Secondly, the response of the ESO must be as soon as possible, so as to obtain the estimation of states and disturbances quickly. The bandwidth should not be smalller than sampling frequency of angular postion.

It should be pointed out that a nonlinear ESO can also be used to estimate the disturbances[24]. The advantages of nonlinear ESO are that it may obtain a better observation precision and a faster converging estimation. However, it needs to tune more parameters to ensure the estimation performance.

3.2 ADRC

Usually, a practical structure of cascade control loops for PMSM motion control system includes a loop of position, a loop of speed and two loops of current (as shown in Fig.3). In this paper, we emphasize the design of position controller and speed controller, and assume that the current controllers are properly designed, so that the gain of current loop is set to 1.

With the linear ESO (7) properly designed, its outputs will track the states x_1, x_2 and disturbance $a(t)$, respectively. So a feed forward compensation for the disturbance $a(t)$ can be employed immediately in the control design. The structure of linear ADRC based on ESO for PMSM motion control system is shown in Fig.4. The controller is given by

$$u = \frac{-z_3 + u_0}{b_0} \tag{13}$$

Equation (13) demonstrates the key idea of ADRC: the control of complex, nonlinear, time-varying, and uncertain process in (6) is reduced to a simple problem by a direct and active estimation and rejection of the generalized disturbance.

Ignoring the estimation error in z_3, that is, $z_3 = a(t)$, the plant is reduced to a unit gain double integrator,

$$\ddot{y} = a(t) + b_0 u = \left(a(t) - z_3\right) + u_0 \approx u_0 \tag{14}$$

From (14), we can see that all disturbances are compensated completely. The plant (14) is easily controlled with a PD controller,

$$u_0 = k_p\left(\theta_m^* - z_1\right) - k_d z_2 \tag{15}$$

Where θ_m^*, z_1 and z_2 are the set point of angular position, estimations of mechanical angular positon and mechanical angular velocity, respectively. Note that $-k_d z_2$, instead of $k_d(d\theta_m^*/dt - z_2)$, is used to avoid differentiation of the set point and to make the closed-loop transfer function pure second order without a zero:

$$G_{cl} = \frac{k_p}{s^2 + k_d s + k_p} \tag{16}$$

Here, the gains can be selected as

$$k_d = 2\xi\omega_c, \text{ and } k_p = \omega_c^2 \tag{17}$$

where ω_c and ξ are the desired closed loop natural frequency and damping ratio. ξ is selected to avoid any oscillations.

From the discussion above, we can get some useful conclusions.

1) Since the design of linear ADRC is based on the ESO, the performance of ADRC is largely dependent on that of ESO. As the ESO is located in the feedback channel, any estimation error would result in the steady-states error which cannot be overcome by the controller. In addition, the

characteristic of robustness of the ADRC would be lost.

2) In the ESO-based linear ADRC, a PD controller achieves zero steady state error without using an integrator. So the dynamic response of ADRC is faster than that of traditional PID controller. It is worth to note that, the PD controller in (15) can be replaced with a more elaborate loop-shaping design, if necessary.

3) The design of ADRC is model independent. Once the ESO is set up, the performance of ADRC is quite insensitive to the model variations and other disturbances. The only parameter needed is the approximate value of b_0 in (4), which is an estimate of K_T/J_n. There are many methods to identify the inertia moment of the plant.

In fact, by using different linear gain combinations in the ESO and the feedback, one can easily find many different controllers in the same ADRC structure. Regardless of which one of these control laws is chosen, the controller coefficients are not dependent on the mathematical model of the plant, thus making ADRC largely model independent. These coefficients are primarily functions of the "time scale," i.e., how fast the plant changes. That is, the controller only needs to act as fast as the plant can react, and this is implicitly represented by the choice of the sampling period.

4) The combined effects of the unknown disturbance and the internal dynamics are treated as a generalized disturbance. By augmenting the observer to include an extra state, it is actively estimated and canceled out, thereby achieving active disturbance rejection.

3.3 Estimation of b_0

As discussed above, the performance of ESO-based linear ADRC applied in the PMSM motion control system is largely dependent on the precise and fast response of the ESO. The parameter, b_0, an approximate value of K_t/J_n, is vital for the ESO. However, in most applications, the real value of b_0 can not be obtained. Since the torque coefficient K_t that is related to rotor flux is changed slowly as the operating of system, it is considered to be constant in this paper. Therefore, the value of b_0 is determined mainly by the inertia of system, which varies when the PMSM drives different load devices that have different inertias. The variation of load will degrade the performance of the ADRC, and in some extreme circumstances, the whole control system will be unstable if the approximate value of b_0 is fixed to a constant value.

Table1 Parameters of the PMSM

Rated power (kW)	1.0
Poles	10
Rated torque (Nm)	4.77
Rated phase current (A)	5.7
Torque coefficient	0.47
Rated speed (rpm)	2000
Phase resistance (Ω)	0.452
Phase inductance (mH)	4.2
Inertia moment (10^{-4}kgm^2)	4.44

Next, we will show this phenomenon by simulation results. The parameters of the PMSM used in the simulation are shown in Table 1. Here, in the simulation, the poles of ESO are all assigned to -10. Parameters of the PD controller, k_p and k_d, are set to 987 and 62.4, respectively.

Fig.5 and Fig.6 show the step responses of the ADRC controller. In Fig.5, the value of b_0 is fixed to K_t/J_m, 1058.5, while the inertial moments of system are assigned to J_m, $5J_m$ and $10J_m$, respectively. In Fig.6, the inertial moment of system is fixed to $5J_m$, while the value of b_0 is changed.

From the simulation results, we can see that the performance of the ADRC controller will be diminished if the inertia of the whole system varies largely and the controller does not have any adaptation ability to handle this kind of changes. In fact, when the inertia of the system is increased, K_t/J_n becomes smaller, and b_0 should become smaller accordingly. However, if b_0 is fixed to be a constant $b_0 = K_t/J_m$, when the inertia of the system is increased, neither the control term i_q^* nor b_0 changes, then the term $b_0 i_q^*$ becomes bigger and makes ω become bigger according to (5). At last, the performance of whole system is deteriorated. To improve the control system, the $b_0 i_q^*$ term should correspondingly be decreased, i.e., b_0 should be reduced when the inertia of the system is increased.

So in order to get a higher performance drive, the inertia of the system should be identified, and b_0 should be adjusted according to the variation of system inertia. There are many methods to identify the value of system inertia. Here we use the method introduced in [25] to identify the load inertia.

$$\Delta J_n(k) = -\frac{\lim_{k\to\infty}\int_{(k-1)T}^{kT} \hat{T}_d \cdot \dot{q}_1 \, dt}{\lim_{k\to\infty}\int_{(k-1)T}^{kT} \dot{q}_1^2 \, dt}, k = 1, 2... \quad (18)$$

$$\hat{J}_n = \Delta J_n + J_n \quad (19)$$

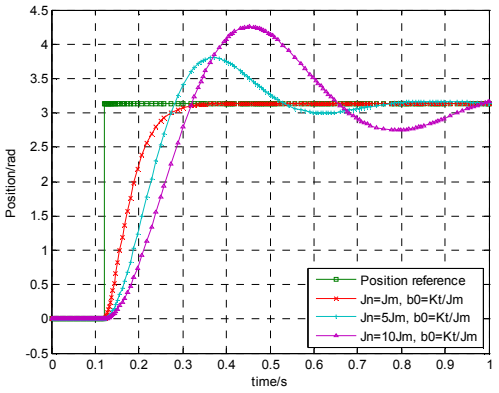

Fig.5 Step responses of ADRC when the inertial memont of system increases

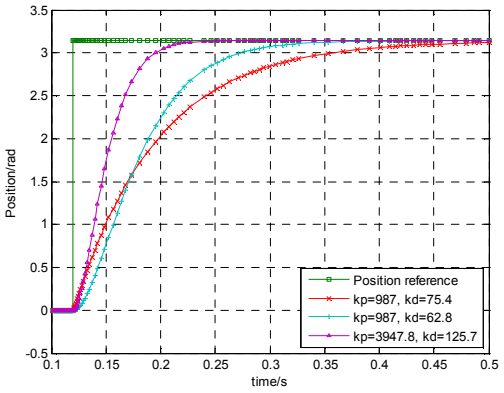

Fig.8 Step responses of ADRC with different PD controllers

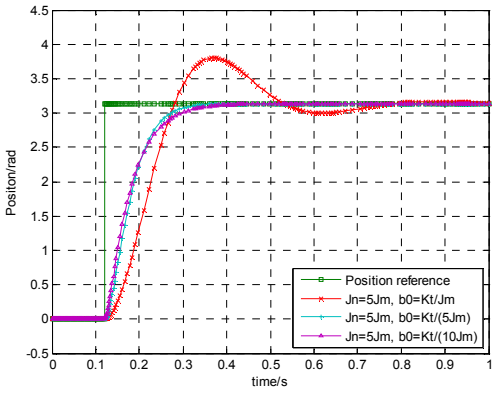

Fig.6 Step responses of ADRC when inertial moment of system is fixed and b_0 is changed

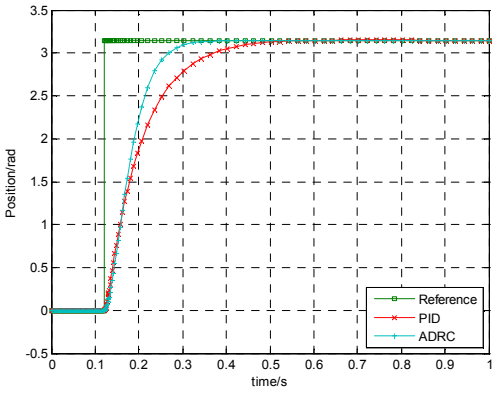

Fig.9 Comparation of ADRC controller and normal PID controller, J_n=J_m

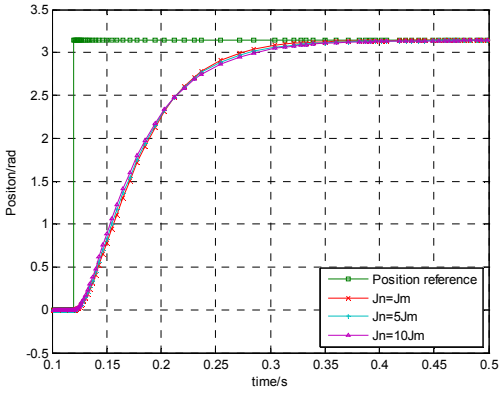

Fig.7 Performance of ADRC when b_0 is adjusted according to the inertial moment of system

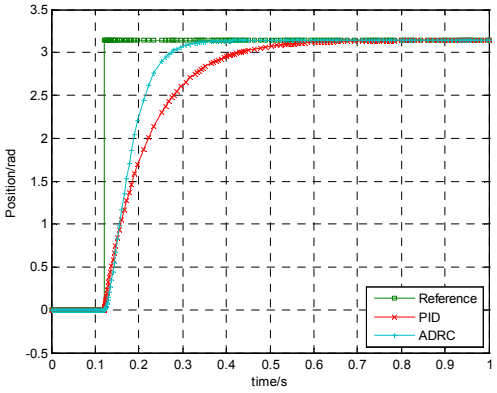

Fig.10 Comparation of ADRC controller and normal PID controller, J_n=$10J_m$

where $\Delta J_n(k)$ is k-th sampled increment of inertia, $\hat{J}_n$ is the estimation of system inertia, and q_1 satisfies

$$\frac{dq_1}{dt} = -\lambda q_1 + \lambda \omega_r, q_1(0) = 0 \qquad (20)$$

$\lambda > 0$, $-\lambda$ is the pole of observer.

Once the inertial moment of system is identified, b_0 is changed correspondingly. Fig.7 shows the performance of the ADRC controller when b_0 is adjusted according to the inertial moment of system. We can see that, the ADRC controller works well at different situations. Fig.8 shows step responses of ADRC with diffenent PD controllers. From the simulation results, we can conclude that, once the ESO is set up, the performance of ADRC is mainly

dependent on k_p and k_d, which are easily determined by the desired closed loop natural frequency and damping ratio.

3.4 Comparation Study

A comparation study between ADRC controller and normal PID controller is carried out. Two PMSM motion systems are established in MATLAB/ SIMULINK. One is implemented with ADRC controller, and the other one is implemented with PID contoller. The specifications of PMSMs used in simulation are the same as that shown in Table 1. Current loops of the both systems are set to unit gain. Other parameters of PID controller are given as follow: speed-loop proportional is 94.4, speed-loop integral gain is 214.7, and position-loop proportional gain is 10. Parameters of ADRC controller are selected as: k_p is 987, and k_d is 62.4. A step signal is used as position reference. The responses of both systems with different loads are shown in Fig.9 and Fig.10. Both controllers perform well but ADRC yields smaller error and faster response. It is worthy to note that, increasing the position-loop proportional gain will induce faster response. However, an overshoot will generate, which is not allowed in some applications.

4 Experimental Verification

4.1 Experimental System

The hardware schematic of experimental system is shown in Fig.11. A surface PMSM is used in the experiment and Tabel1 gives the parameters of the PMSM. The PMSM is driven by a three-phase current controlled PWM inverter. The inverter is implemented by the Intelligent Power Module (IPM) including gate drives, six-IGBTs and protection circuits. The rotor position is measured by means of 2500-pulse/revolution encoder. A programable logical device FPGA XC3S50AN is used at the encoder interface to process outputs of the encoder. Vector-controlled PMSM drive incorporated with the proposed control scheme is experimentally implemented using TI DSP TMS320F2812. The new TMS320F2812 is the industry's 32-bit control DSP with on-board flash memory and performance up to 150 MIPS. It's designed specially for industry control applications.

The structrue of whole control system in the test includes a linear ESO, an ESO-based linear ADRC

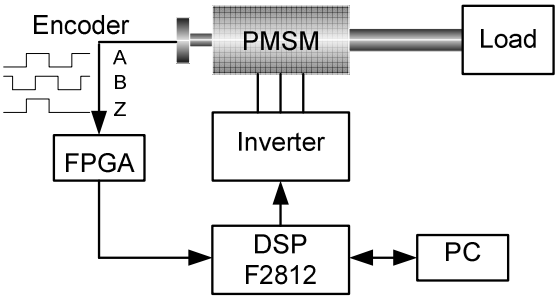

Fig.11 Configuration of the experiment system

and two current loops. The current control loops are realized by two PID controller with parameters well tuned. Since this paper emphasizes the design and performance of ADRC, the tuning method of current contol loops is not discussed.

Since the linear ESO mentioned in Section 3.1 is vital for ADRC, the method how to implement the ESO in DSP is discussed detailedly in the following section. Moreover, in order to obtain angular position precisely in the situation of low speed, an asynchronous sampling method (ASM) is employed.

4.2 Implementation of ESO

The ESO (7) is a full observer, which can reconstruct all the state variables. In order to illustrate how to implement the ESO, write (7) in discrete form,

$$\mathbf{z}[n+1]=\mathbf{A_d}\mathbf{z}[n]+\mathbf{B_d}u[n]+\mathbf{L_d}\left(y[n]-\hat{y}[n]\right) \quad (21)$$

where

$$\mathbf{z}[n]=\left[\hat{\theta}_m[n] \quad \hat{\omega}_m[n] \quad \hat{a}[n]\right]^T,$$

$$\mathbf{A_d}=\left[\begin{array}{c|cc}\mathbf{A_{d11}} & \mathbf{A_{d12}}\\ \hline \mathbf{A_{d21}} & \mathbf{A_{d22}}\end{array}\right]=\left[\begin{array}{c|cc}1 & T_1 & T_1^2/2\\ \hline 0 & 1 & T_1\\ 0 & 0 & 1\end{array}\right],$$

$$\mathbf{B_d}=\left[\begin{array}{c}\mathbf{B_{d1}}\\ \hline \mathbf{B_{d2}}\end{array}\right]=\left[\begin{array}{c}b_0T_1^2/2\\ \hline b_0T_1\\ 0\end{array}\right] \quad \mathbf{L_d}=\left[\begin{array}{c}\mathbf{L_{d1}}\\ \hline \mathbf{L_{d2}}\end{array}\right]=\left[\begin{array}{c}l_1T_1\\ \hline l_2T_1\\ l_3T_1\end{array}\right]\triangleq\left[\begin{array}{c}l_{d1}\\ \hline l_{d2}\\ l_{d3}\end{array}\right],$$

and T_1 is the control sampling period, 100us.

While in practice, the state of angular position may be obtained directly and accurately from the encoder, so that a reduced-order observer is suitable, wherein the remaining state variables ω_m, $a(t)$ are to be observed. For clarity herein, z_1 is replaced by $\theta[n]$. From (21) a reduced-order observer becomes

$$\begin{aligned}\mathbf{z}_2[n+1]&=\left(\mathbf{A}_{d22}-\mathbf{L}_{d2}\mathbf{A}_{d12}\right)\mathbf{z}_2[n]\\&+\mathbf{L}_{d2}\left(\hat{\theta}_m[n+1]-\hat{\theta}_m[n]-\mathbf{B}_{d1}u[n]\right)+\mathbf{B}_{d2}u[n]\end{aligned} \quad (22)$$

where

$\mathbf{z}_2[n]=\left[\hat{\omega}_m[n] \quad \hat{a}[n]\right]^T$.

The minimum-order observer for angular velocity and total disturbance requires only the current and previous sample angular position as provided by the encoder, along with the known *q*-axis current.

Using (21) and measured information of angular position and q-axis current, $\theta_m[n]$, $u[n]$, an estimated value of angular position based on $\omega_m[n]$, $a[n]$ can be written as

$$\hat{\theta}_m[n+1]=\hat{\theta}_m[n]+\begin{bmatrix}T_1 & T_1^2/2\end{bmatrix}\begin{bmatrix}\omega_m[n]\\ a[n]\end{bmatrix}+\frac{b_0u[n]T_1^2}{2} \quad (23)$$

Defining estimation error

$\Delta\theta_m[n+1]\equiv\hat{\theta}_m[n+1]-\theta_m[n+1]$,

(23) can be rearranged as

$$\hat{\theta}_m[n+1]=-\Delta\theta_m[n+1]+\hat{\theta}_m[n]+\begin{bmatrix}T_1 & T_1^2/2\end{bmatrix}\begin{bmatrix}\omega_m[n]\\ a[n]\end{bmatrix}+\frac{b_0uT_1^2}{2} \quad (24)$$

with (24), (22) can be written as

$$\mathbf{z}_2[n+1]=\mathbf{A}_{d22}\mathbf{z}_2[n]-\mathbf{L}_{d2}\Delta\theta_m[n+1]+\mathbf{B}_{d2}u[n] \quad (25)$$

Formula (22) is the final form of the ESO used in this paper.

In real applications, actual angular position $\theta_m[n]$ is detected by counting the number of encoder pulse. In the high or middle speed region, the angular position can be obtained immediately and accurately, so the ESO works perfectly. However, in spite of the high precision encoder, a pulse interval becomes longer than the control sampling interval in a very low speed region and occasionally only one pulse income into several sampling intervals (as shown in Fig.1). In such case, there are positioning error and detection delay between the actual angular position and that detected by the ESO. The error and delay will deteriorate the performance of the ESO. To address this problem, a method denoted as asynchronous sampling method (ASM) is developed in the following section.

4.3 Asynchronous Sampling Method

The ASM has two sampling rate for angular position. In the high or middle speed region, the angular position θ_m[n] is forced to be synchronized with control sampling period, T_1. While in the low speed region, the angular position is forced to be synchronized with encoder pulse interval. At the moment of an encoder pulse input, the estimates $\mathbf{z_2}$ are updated by $\Delta\theta_m$. Between these long sample updates, at each new short T_1 control sampling instant, angular position θ_m and angular velocity ω_m are estimated, while disturbance $a(n)$ is assumed constant. The process of calculation is illustrated as follow.

As shown in Fig.1, at the moment of m-th encoder pulse input, the actual angular position is $\theta_m[m]$ and the estimated value is given by

$$\hat{\theta}_{maux}[n]=\hat{\theta}_m[n]+\hat{\omega}_m[n]T_{aux}[n]+T_{aux}^2[n]\left(\hat{a}[n]+b_0u[n]\right)/2 \quad (26)$$

$T_{aux}[n]$ is the interval between the latest n-th control sampling and m-th encoder pulse. It's easily obtained by a simple hardware logical device, such as FPGA. Then we can obtain the estimation error

$$\Delta\theta_{maux}[n]=\hat{\theta}_{maux}[n]-\theta_m[m] \quad (27)$$

Yield $\Delta\theta_{maux}[n]$ as input to (25) to improve the estimates for $\omega_{maux}[n]$ and $a_{aux}[n]$.

$$\hat{\omega}_{maux}[n]=\hat{\omega}_m[n]+\left(\hat{a}[n]+b_0u[n]\right)T_{aux}-l_{d2}\Delta\theta_{maux}[n] \quad (28)$$

$$\hat{a}_{aux}[n]=\hat{a}[n]-l_{d3}\Delta\theta_{maux}[n] \quad (29)$$

At the instant of control sample immediately after the encoder pulse, the estimator uses the actual $\theta[m]$ and estimated $\omega_{raux}[n]$ as the old state, and updates the new estimate as

$$\begin{aligned}\hat{\theta}_m[n+1]&=\theta_m[m]+\hat{\omega}_{maux}[n]\left(T_1-T_{aux}[n]\right)\\&\quad+\left(T_1-T_{aux}[n]\right)^2\left(\hat{a}_{aux}[n]+b_0u[n]\right)/2\end{aligned} \quad (30)$$

$$\hat{\omega}_m[n+1]=\hat{\omega}_{maux}[n]+\left(\hat{a}_{aux}[n]+b_0u[n]\right)\left(T_1-T_{aux}\right) \quad (31)$$

4.4 Experimental Results and Discussion

In order to check the performance of ADRC, a unit step position command of 3.14rad is applied at t=0.12s. The inertia moment of load is 4×10^{-4}kgm^2.

Fig.12 shows the measured responses with different k_p and k_d. It is clear that the steady state error of the tracking response is zero, although there is no integrator. Forthurmore, the performance of the entire system is decided by k_p and k_d, and is independent on the model. Increasing k_p and k_d will induce faster tracking response. But there will be an overshoot if k_p and k_d are too large. In the real applications, k_p and k_d can be set according to the control sampling time and the entire inertia moment of motion system.

Fig.13 shows the tracking responses of PMSM drive incorporated with ADRC and PID controller, respectively. The parameters of ADRC controller and PID controller are the same as that specified in 3.4. Since a PD controller is used instead of a PI controller in ADRC, the dynamic response of ADRC is faster than that of traditional PID controller.

Fig.14 shows the results of ESO used synchronous sampling method (SSM) and asynchronous

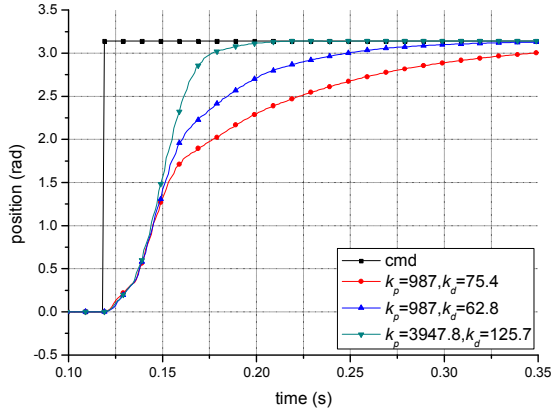

Fig.12 Tracking responses of PMSM drive incorporated with ADRC.

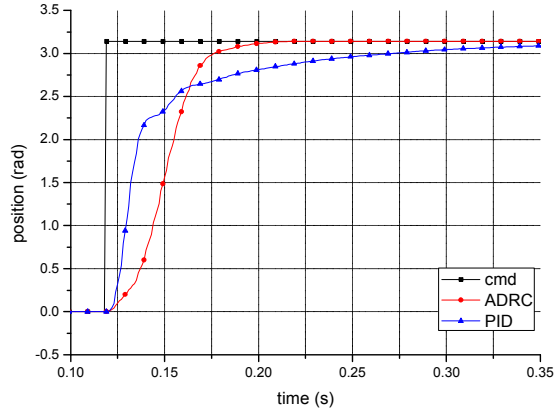

Fig.13 Tracking responses of PMSM drive incorporated with ADRC and traditional PID controller, respectively.

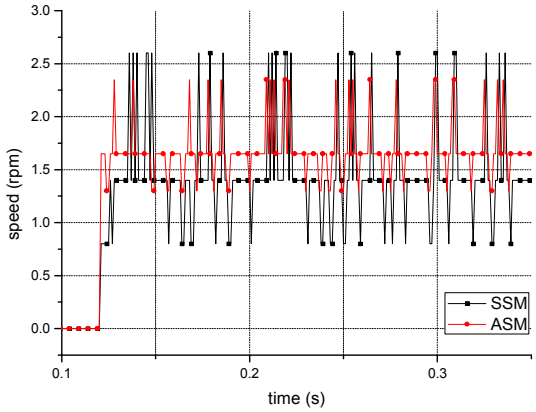

Fig.14 Results of ESO in low speed region.

sampling method (ASM) in the low speed region. In this experiment test, a rample position command of (πt)/15rad is applied at t=0.12s. So the speed reference is 2rpm. The estimation errors of ESO usd SSM and ASM are ±1.2rpm and ±0.7rpm, respectively.

5 Conclusions

In the real motion applications, there are many disturbances, which make it difficult to obtain a sufficiently high performance for PMSM motion control systems in the entire operating range. Furthermore, since the angular position is detected by counting the pulses of encoder, there are positioning error and detection delay between the actual angular position and the measured value in the low speed region. To address these issues, a novel active disturbance rejection control scheme has been proposed in this paper. A linear ESO is used to estimate all the disturbances, and then make the corresponding compensation in a linear ADRC. The ESO-based linear ADRC is model independent. It achieves zero steady state error using a PD controller instead of an integrator. In the linear ADRC, the combined effects of the unknown disturbance and the internal dynamics are treated as a generalized disturbance. By augmenting the observer to include an extra state, it is actively estimated and canceled out, thereby achieving active disturbance rejection. When the PMSM operates in a low speed region, an ASM is used to obtain the accuracy angular position. Experimental results have shown that the proposed method achieves a good performance in the presence of disturbances and the entire operating range.

References:

[1] P. Cominos and N. Munro, PID controllers: recent tuning methods and design to specification, *Control Theory and Applications, IEE Proceedings* -, Vol. 149, No.1, 2002, pp. 46-53.

[2] L. H. Keel, J. I. Rego, and S. P. Bhattacharyya, A new approach to digital PID controller design, *Automatic Control, IEEE Transactions on*, Vol. 48, No. 4, 2003, pp. 687-692.

[3] A. Kiam Heong, G. Chong, and L. Yun, PID control system analysis, design, and technology, *Control Systems Technology, IEEE Transactions on*, Vol. 13, No. 4, 2005, pp. 559-576.

[4] S. Jianbo, Q. Wenbin, M. Hongyu, and W. Peng-Yung, Calibration-free robotic eye-hand coordination based on an auto disturbance-rejection controller, *Robotics, IEEE Transactions on*, Vol. 20, No.5, 2004, pp. 899-907.

[5] S. Piccagli and A. Visioli, Minimum-time feedforward technique for PID control, *Control*

Theory & Applications, IET, Vol. 3, No. 10, 2009, pp. 1341-1350.

[6] Y. A. R. I. Mohamed and T. K. Lee, Adaptive self-tuning MTPA vector controller for IPMSM drive system, *Energy Conversion, IEEE Transactions on*, Vol. 21, No. 3, 2006, pp. 636-644.

[7] K. Ying-Shieh and T. Ming-Hung, FPGA-Based Speed Control IC for PMSM Drive With Adaptive Fuzzy Control, *Power Electronics, IEEE Transactions on*, Vol. 22, No. 6, 2007, pp. 2476-2486.

[8] K. Seok-Kyoon, Speed and current regulation for uncertain PMSM using adaptive state feedback and backstepping control, *IEEE International Symposium on Industrial Electronics*, 2009, pp. 1275-1280.

[9] S. Kuo-Kai, L. Chiu-Keng, T. Yao-Wen, and I. Y. Ding, A newly robust controller design for the position control of permanent-magnet synchronous motor, *Industrial Electronics, IEEE Transactions on*, Vol. 49, No. 3, 2002, pp. 558-565.

[10] S. Jianbo, M. Hongyu, Q. Wenbin, and X. Yugeng, Task-independent robotic uncalibrated hand-eye coordination based on the extended state observer, *Systems, Man, and Cybernetics, Part B: Cybernetics, IEEE Transactions on*, Vol. 34, No. 4, 2004, pp. 1917-1922.

[11] Y. Lin-Ru, M. Zhen-Yu, W. Xiao-Hong, and Z. Hao, Sliding mode control for permanent-magnet synchronous motor based on a double closed-loop decoupling method, *Proceedings of the Fourth International Conference on Machine Learning and Cybernetics*, 2005, pp.1291-1296.

[12] S. Jayasoma, S. J. Dodds, and R. Perryman, A FPGA implemented PMSM servo drive: practical issues, *Universities Power Engineering Conference*, 2004, pp. 499-503.

[13] H. Hahn, A. Piepenbrink, and K. D. Leimbach, Input/output linearization control of an electro servo-hydraulic actuator, *Proceedings of the Third IEEE Conference on Control Applications*, 1994, pp. 995-1000.

[14] J. Hu, Y. Xu, and J. Zou, Design and Implementation of Adaptive Backstepping Speed Control for Permanent Magnet Synchronous Motor, *The Sixth World Congress on Intelligent Control and Automation*, 2006, pp. 2011-2016.

[15] S. S. Wankun Zhou, Zhiqiang Gao, A Stability Study of the Active Disturbance Rejection Control, *Applied Mathematical Sciences*, Vol. 3, No. 10, 2009, pp. 491 - 508.

[16] B. Porter, Issues in the design of intelligent control systems, *Control Systems Magazine, IEEE*, Vol. 9, No. 1, 1989, pp. 97-99.

[17] H. Hui-Min, An architecture and a methodology for intelligent control, *IEEE Expert*, Vol. 11, No. 2, 1996, pp. 46-55.

[18] J. W. Choi, S. C. Lee, and H. G. Kim, Inertia identification algorithm for high-performance speed control of electric motors, *Electric Power Applications, IEE Proceedings* -, Vol. 153, No. 3, 2006, pp. 379-386.

[19] K. Euntai and L. Sungryul, Output feedback tracking control of MIMO systems using a fuzzy disturbance observer and its application to the speed control of a PM synchronous motor, *Fuzzy Systems, IEEE Transactions on*, Vol. 13, No. 6, 2005, pp. 725-741.

[20] Y. A. R. I. Mohamed, Design and Implementation of a Robust Current-Control Scheme for a PMSM Vector Drive with a Simple Adaptive Disturbance Observer, *Industrial Electronics, IEEE Transactions on*, Vol. 54, No. 4, 2007, pp. 1981-1988.

[21] C. Young-Kiu, L. Min-Jung, K. Sungshin, and K. Young-Chul, Design and implementation of an adaptive neural-network compensator for control systems, *Industrial Electronics, IEEE Transactions on*, Vol. 48, No. 2, 2001, pp. 416-423.

[22] J. Q. Han, Auto-disturbance-rejection control and its applications, *Control Desision*, Vol. 13, No. 1, 1998, pp. 19-23.

[23] G. Zhiqiang, Scaling and bandwidth -parameterization based controller tuning, *Proceedings of the American Control Conference*, 2003, pp. 4989-4996.

[24] G. Zhiqiang, H. Shaohua, and J. Fangjun, A novel motion control design approach based on active disturbance rejection, *Proceedings of the 40th IEEE Conference on Decision and Control,* 2001, pp. 4877-4882.

[25] I. Awaya, Y. Kato, I. Miyake, and M. Ito, New motion control with inertia identification function using disturbance observer, *Power Electronics and Motion Control, Proceedings of the 1992 International Conference on Industrial Electronics, Control, Instrumentation, and Automation*, 1992, pp. 77-81.